future internet

MDPI

Article

System Performance Analysis of Sensor Networks for RF Energy Harvesting and Information Transmission

Kuncheng Lei [1,*] and Zhenrong Zhang [2]

[1] School of Computer, Electronics and Information, Guangxi University, Nanning 530004, China
[2] Guangxi Key Laboratory of Multimedia Communications and Network Technology, School of Computer, Electronics and Information, Guangxi University, Nanning 530004, China
* Correspondence: 2013591028@st.gxu.edu.cn; Tel.: +86-15078774797

Abstract: This paper investigates the problem of RF energy harvesting in wireless sensor networks, with the aim of finding a suitable communication protocol by comparing the performance of the system under different protocols. The network is made up of two parts: first, at the beginning of each timeslot, the sensor nodes harvest energy from the base station (BS) and then send packets to the BS using the harvested energy. For the energy-harvesting part of the wireless sensor network, we consider two methods: point-to-point and multi-point-to-point energy harvesting. For each method, we use two independent control protocols, namely head harvesting energy of each timeslot (HHT) and head harvesting energy of dedicated timeslot (HDT). Additionally, for complex channel states, we derive the cumulative distribution function (CDF) of packet transmission time using selective combining (SC) and maximum ratio combining (MRC) techniques. Analytical expressions for system reliability and packet timeout probability are obtained. At the same time, we also utilize the Monte Carlo simulation method to simulate our system and have analyzed both the numerical and simulation solutions. Results show that the performance of the HHT protocol is better than that of the HDT protocol, and the MRC technology outperforms the SC technology for the HHT protocol in terms of the energy-harvesting efficiency coefficient, sensor positions, transmit signal-to-noise ratio (SNR), and length of energy harvesting time.

Keywords: energy harvesting; wireless sensor networks; system reliability; packet timeout probability; outage probability

Citation: Lei, K.; Zhang, Z. System Performance Analysis of Sensor Networks for RF Energy Harvesting and Information Transmission. *Future Internet* **2023**, *15*, 172. https://doi.org/10.3390/fi15050172

Academic Editors: Chan Hwang See, Simeon Keates, Yousef Dama, Kelvin Anohm and Raed A. Abd-Alhameed

Received: 7 April 2023
Revised: 27 April 2023
Accepted: 29 April 2023
Published: 30 April 2023

1. Introduction

Wireless communication has attracted substantial attention in recent years as a promising field of research due to its versatility and economic benefits, particularly with the advent of sixth-generation (6G) communications. As a result, wireless sensor networks have found extensive applications in various aspects of our lives, such as medical, industrial manufacturing, and the Internet of Things (IoT) [1–4]. However, there are still issues that need to be addressed in wireless communication systems, such as equipment service life, complex environments, and the impact of channel states on energy harvesting and information transmission [5,6].

The topic of energy harvesting is constantly in the news, as we need energy in all aspects of our lives. While renewable energy sources such as wind, solar, and hydraulic potential are frequently used, some devices, such as artificial hearts and forest monitoring systems, cannot easily compensate for the lack of energy. Therefore, radio frequency (RF) wireless energy harvesting and usage have become a primary research topic in these fields. In an RF wireless energy harvesting system, the uplink information transfer and the downlink wireless energy harvesting are limited, leading to unsatisfactory system performance and restrictions [7]. Therefore, it is essential to distribute the time for sending packets and energy harvesting consistently to reduce the impact on system performance [8].

Energy-harvesting technologies have shown great potential in powering small electronic devices without the need for external power sources. However, existing energy-harvesting devices suffer from large size and low power conversion efficiency. To address these challenges, a better approach to energy harvesting was proposed in paper [9], that is, metasurfaces and metamaterial structures are proposed as collectors for energy-harvesting devices that provide higher conversion efficiency in smaller sizes. One such example is the bow-tie multi-band rectenna with slots proposed in a paper by Agrawal et al. This rectenna is designed for ambient wireless energy harvesting for autonomous IoT sensors, featuring a high-conversion-efficiency multi-band rectification circuit composed of four single-ring rectifiers. The paper also proposes a power management circuit to store and convert the harvested voltage, smoothing the direct current (DC) output voltage and improving system performance [10].

The design of energy-harvesting devices must meet certain standards to ensure optimal system performance. In this regard, Wagih et al. divided the rectenna into antenna rectification impedance bandwidth and antenna radiation characteristics, in accordance with wireless power transfer (WPT) and antenna design for environmental RF energy harvesting application standards [11]. In another paper, the non-orthogonal multiple access (NOMA) protocol is studied to transmit IoT relay node data together with source node data in the presence of interfering signals. The outage probability, throughput and total throughput are mathematically derived, and a representative performance comparison method is given [12]. Finally, a paper by Liu et al. presents the design of a three-band high-gain multi-beam ambient RF energy-harvesting system utilizing hybrid combination. This system maximizes the use of harvested RF energy by utilizing frequency, space, and polarization simultaneously. A broadband hybrid combination is proposed that enables energy harvesting at low RF power densities while maintaining the wide frequency and spatial coverage required for ambient RF energy harvesting [13]. In paper [14], the limited sensitivity and nonlinearity of far-field RF energy harvesting are presented and their effects quantified. Furthermore, a linear model and two nonlinear models are proposed, and the differences in wireless information and power transfer designs for each model are shown in single-user and multi-user deployments [15].

RF energy-harvesting technology is widely used in the Internet of Things, and many advanced energy harvesting technologies have been proposed in these applications [16–19]. RF energy-harvesting systems face two significant challenges: system reliability and packet timeout probability. To address these problems, researchers have proposed several solutions, including improving system performance in wireless sensor networks through the Low-Energy Adaptive Clustering Hierarchy (LEACH) protocol [20] and analyzing interrupt performance in wireless sensor networks [21]. In particular, Tran proposed a system performance research method in [22] using two energy-harvesting protocols: the head harvesting energy of each timeslot (HHT) and the head harvesting energy of a dedicated timeslot (HDT). Researchers can choose a protocol that is more suitable for communication by contrasting the system performance of the HHT protocol under maximal ratio combining (MRC) and selection combining (SC) techniques with the HDT protocol under MRC and SC technology. According to [22], the HDT protocol harvests energy during a designated time slot, whereas the HHT protocol harvests energy at the head of the time slot. The energy-harvesting time is $\alpha_0 T$ and $\alpha_{0k} T$, and $\alpha_0 = K\alpha_{0k}$, where K is the number of sensor nodes. The size of the transmitted packets is the same for both the HHT and HDT protocols in paper [22], where the size of the packet transmitted by the system is set to L. Given that the HDT protocol harvests energy over a significantly longer period than the HHT protocol, this can lead to an unfavorable contrast. Moreover, the complex channel characteristics that apply to both MRC and SC technology are not taken into account in study.

In response, we reformulate the optimization problem put out in [22] in order to solve these problems, and we offer competitive energy-harvesting strategies in this reformulated problem. To determine which protocol is best for the energy-harvesting system, different packet sizes are assigned to various protocols, and then, they are compared once more. The

research findings of paper [22] show that the HDT protocol performs better than the HHT protocol. Our improved simulation results, however, show that HHT performs better and is more suited for RF wireless communication, particularly the HHT protocol using MRC technology. It is appropriate, and the following analysis provides a detailed examination.

2. System and Channel Model

In this section, we present our suggested system model, along with a comprehensive explanation of the HHT and HDT protocols.

2.1. System Model

In our system, both the HDT and HHT protocols utilize time division multiplexing technology. We assume that the channel variation between any two sensor nodes and the BS follows Rayleigh block fading and is affected by additive white Gaussian noise. We also assume that the channel state remains unchanged during a fixed period of energy harvesting and packet transmission, and that each transmission time is relatively independent. Rayleigh fading has been widely accepted as a reasonable signal propagation model and an effective model for complex environments. Given the complexity of our environment, we have chosen to model the channel fading between the sensor nodes and the BS in our system using the Rayleigh communication model. After conducting a rigorous analysis, we have considered a relatively reasonable system model, as shown in Figure 1. Our system model comprises a BS and multiple sensor nodes N_k that are responsible for both energy harvesting and information transmission. These nodes harvest energy from the BS and use it to transmit packets to the BS, thus completing the system model. To optimize the energy harvesting and information transmission processes, we install $M + 1$ antennas for the BS. M antennas are used for uplink data packet transmission, while the remaining antenna is dedicated to downlink energy harvesting, which enables the BS to obtain energy from the nodes.

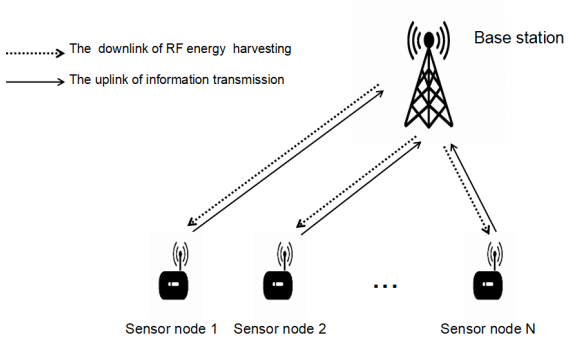

Figure 1. Wireless power communication system model. The dotted line is used for downlink energy harvesting, and the solid line is arranged for uplink packet transmission.

In our system, we have information transmission in the uplink and energy harvesting in the downlink. We use G_{k1j} to represent the channel gain of the uplink information transmission process from sensor node N_k to the base station (BS), where $\forall k \in \{1, 2, \ldots, K\}$ and $\forall j \in \{1, 2, \ldots, M\}$. Similarly, we use G_{k2j} and G_{k3j} to denote the channel gain of energy harvesting for the HDT and HHT protocols, respectively, i.e., the channel gain of downlink energy harvesting. Since the channel state change is random, we model the channel gain of the system as a random variable that follows the exponential distribution. As a result, based on the concepts of probability density function (PDF) and cumulative distribution function (CDF), we can define the PDF and CDF of the channel gain as follows:

$$f_X(x) = \frac{1}{\theta_k} Exp(-\frac{x}{\theta_k}), \tag{1}$$

$$F_X(x) = 1 - Exp(-\frac{x}{\theta_k}), \tag{2}$$

where X is a random variable about the channel gain, and θ_k is the average channel gain of the random variable X. In this system, the channel mean gains of random variables G_{k1}, G_{k2} and G_{k3} are represented by ω_k, Θ_k and Φ_k, respectively.

2.2. HDT Protocol

The protocol uses the time division multiple access (TDMA) method, as shown in Figure 2. The time T is divided into $K+1$ segments. During the first segment, the sensor nodes harvest energy from the BS, which then allocates K time slots to the sensor nodes for transmitting packets to the BS. The sum of energy harvesting time and packet transmission time is equal to T, and the expression can be easily derived as

$$\alpha_0 T + \sum_{K=1}^{K} (1-\alpha)_k T = T. \tag{3}$$

The HDT protocol involves two processes for the sensor nodes: first, they must harvest energy from the BS, and then, they can use the harvested energy to transmit packets to the BS. The time required for sensor node N_k to harvest energy from the BS is $\alpha_0 T$ and the energy obtained during this process can be expressed as:

$$E_k = \eta_k P d_k^{-\lambda} G_{k2} \alpha_0 T, \quad \forall k \in \{1, 2, \ldots, K\}, \tag{4}$$

where P denotes the energy harvesting power when the sensor node N_k harvests energy from the BS, η_k is the energy harvesting efficiency index of the energy harvesting process, d is the distance between the sensor node N_k and the BS, and λ is the path loss exponent due to the influence of the randomness of the channel state on the energy harvesting path.

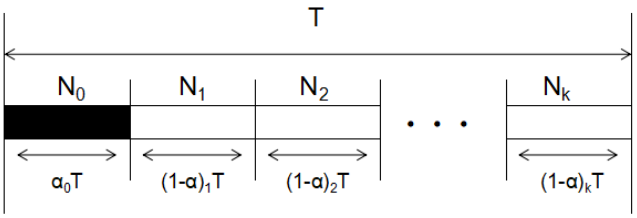

Figure 2. The time required for a node to send a data packet is measured by $(1-\alpha)_k T$, while $\alpha_0 T$ represents the time that all nodes spend together collecting energy.

After energy harvesting, the harvested energy is utilized to send packets to the BS, and the power required for sending packets can be expressed as follows:

$$P_k = \frac{E_k}{(1-\alpha)_k T} = \frac{\alpha_0 P G_{k2} \eta_k d_k^{-\lambda}}{(1-\alpha)_k}. \tag{5}$$

The packet transmission time is the time required for a packet of size L bits to travel from sensor node N_k to the BS; in this case, L denotes L_1 and L_2. The expression is as follows:

$$T_k^{(v)} = \frac{\mathscr{B}_k}{\ln(1+\mu_k \gamma_k^{(v)})}, \tag{6}$$

where $\mathscr{B}_k = \frac{L\ln(2)}{W}$, $\mu_k = -\frac{1}{\log(5*BER_k)}$ [22], W denotes the system bandwidth , while μ_k denotes the bit error rate. We also obtain the expression for the signal-to-noise ratio (SNR), which is as follows:

$$\gamma_k^{(v)} = \frac{P_k G_{k1}^{(v)} d_k^{-\lambda}}{W \mathscr{Q}_0} = \frac{\alpha_0 G_{k1}^{(v)} G_{k2} \gamma_0 \eta_k d_k^{-2\lambda}}{(1-\alpha)_k}, \tag{7}$$

In order to accommodate different downlink energy harvesting methods, we make use of various channel gain assumptions. Specifically, the channel gain $G_{k1}^{(v)}$ utilizes different

technologies depending on the two gain modes, which are represented by G_{k1j} and G_{k2j} for MRC and SC technologies, respectively, and the expression is as follows:

$$G_{k1}^{(v)} = \begin{cases} G_{k1}^{(MRC)} & = \sum_{j=1}^{M} G_{k1j}, \quad v = MRC \\ G_{k1}^{(SC)} & = \max\limits_{j\in\{1,2,\ldots,M\}} G_{k1j}, \quad v = SC, \end{cases} \tag{8}$$

where $\gamma_0 = \frac{P}{W\mathcal{Q}_0}$, $\forall v \in \{MRC, SC\}$.

2.3. HHT Protocol

Similar to the HDT protocol, the total period T is divided into K periods on average, and each period is composed of two parts, which are the time $\alpha_{01}T$ for energy harvesting and the time $(1-\alpha)_k T$ for packet transmission in the HHT protocol, as shown in Figure 3. As a result, the energy harvested by sensor node N_k is as follows:

$$E_k = \alpha_{0k} T P G_{k3} \eta_k d_k^{-\lambda}. \tag{9}$$

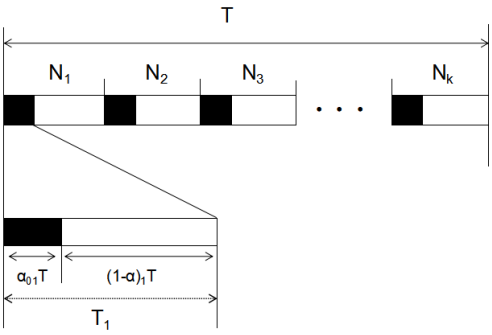

Figure 3. The allocation of energy harvesting time and packet transmission time in the HHT protocol.

After harvesting energy, the sensor nodes use the harvested energy to send packets to the BS. The time spent is $(1-\alpha)_k T$; thus, the sending power is as follows:

$$P_k = \frac{E_k}{(1-\alpha)_k T} = \frac{\alpha_{0k} P G_{k3} \eta_k d_k^{-\lambda}}{(1-\alpha)_k}. \tag{10}$$

The SNR of sensor node N_k sending packets to the BS under the HHT protocol is as follows:

$$\gamma_k^{(v)} = \frac{P_k G_{k1}^{(v)} d_k^{\lambda}}{W\mathcal{Q}_0} = \frac{\alpha_{0k} G_{k1}^{(v)} G_{k3} \gamma_0 \eta_k d_k^{-2\lambda}}{(1-\alpha)_k}. \tag{11}$$

3. Description of System Performance Indicators

We describe the performance metrics discussed in the article in this part, which encompass the performance of both the entire system and a single node.

3.1. Probability of Packet Timeout for Information Transmission between Single Node

A packet transmitted from sensor node N_k to the BS may face a timeout or transmission error due to the complexity of the channel state. We use $T_{k,succ}^{(v)}$ to denote the successful packet transmission event [22], which happens when the time of packet transmission $T_k^{(v)}$ is less than the threshold time $t_{k,out}$. Here, $t_{k,out}$ is the transmission threshold of a packet, and $T_k^{(v)}$ is defined in (6). According to the system definition, the information about the channel condition during both energy harvesting and packet transmission determines the time of packet transmission, which is a random variable. We can rapidly determine the CDF of sensor node N_k transmission time employing the definition of probability as follows:

$$F_{T_k^{(v)}}(t) = \Pr\left\{T_k^{(v)} < t\right\}. \tag{12}$$

In accordance with the channel assumption, we set $t_{out,k} = t_k T = t_{out}$ [22], which denotes that the packet transmission time established by the system is equal to the timeout threshold. In particular, the probability that the packet transmission time is longer than the timeout threshold t_{out} is defined as the packet timeout probability, and the expression is as follows:

$$\mathscr{O}_k^{(v)} = \Pr\left\{T_k^{(v)} \geq t_{out,k}\right\} = 1 - F_{T_k^{(v)}}(t_{out,k}). \tag{13}$$

3.2. Performance Metrics for Complete Systems

In the domain of wireless communication systems, system reliability and outage probability are pivotal performance metrics that have a substantial impact on communication quality. System reliability ensures that the system can maintain a certain level of performance consistently over a prolonged duration, encompassing correct information transmission, stable connection maintenance, and uninterrupted operation. Outage probability measures the probability that the system can sustain the desired communication quality during operation. It can be seen that system reliability and outage probability play a crucial role in determining the overall performance of a wireless communication system, and we will introduce them next.

3.2.1. System Reliability

In wireless sensor networks, system reliability is viewed as the probability that, even under the worst channel conditions, the packet transmission time would not exceed the timeout threshold. The expression is as follows:

$$\mathscr{R}_k^{(v)} = \Pr\left\{T_{\max}^{(v)} < t_{\text{out}}\right\}, \tag{14}$$

where $T_{\max}^{(v)} = \max\limits_{k\in\{1,2,\ldots,K\}}\left\{T_k^{(v)}\right\}$.

3.2.2. Outage Probability

In wireless power sensor networks, the probability that the packet transmission time will surpass the timeout threshold even under ideal channel circumstances is defined as outage probability, and the expression is as follows:

$$\mathscr{O}_{sys}^{(v)} = \Pr\left\{T_{\min}^{(v)} \geq t_{out}\right\}, \tag{15}$$

where $T_{\min}^{(v)} = \min\limits_{k\in\{1,2,\ldots,K\}}\left\{T_k^{(v)}\right\}$. Complying with Lemma 1 from the paper [22], we know that

$$F_{z_k^{(MRC)}}(z) = 1 - \frac{2}{\Gamma(M)}\left(\frac{z}{\theta_k\omega_k}\right)^{\frac{M}{2}} K_M\left(2\sqrt{\frac{z}{\theta_k\omega_k}}\right), \tag{16}$$

$$\begin{aligned} F_{z_k^{(SC)}}(z) = 1 - 2M &\sum_{m=0}^{M-1}\binom{M-1}{m}(-1)^m \\ &\times \sqrt{\frac{z}{(m+1)\theta_k\omega_k}} K_1\left(2\sqrt{\frac{(m+1)z}{\theta_k\omega_k}}\right). \end{aligned} \tag{17}$$

4. System Performance Analysis

In this section, we use the conclusion of Lemma 1 to analyze the HDT and HHT protocols of the systems for consideration.

4.1. The Analysis of the HDT Protocol

4.1.1. Packet Timeout Probability Analysis of Single Node

We can rewrite the CDF of the packet timeout probability by combining (6) with (7), and (12), and the expression is as follows:

$$F_{T_k^{(v)}}(t) = 1 - \Pr\left\{G_{k1}^{(v)} G_{k2} < \left[\exp\left(\frac{\mathscr{B}_k}{t}\right) - 1\right]\mathscr{H}_{k1}\right\}, \tag{18}$$

where $\mathscr{H}_{k2} = \frac{d_k^{-2\lambda}(1-\alpha)_k}{\alpha_0\gamma_0\eta_k\mu_k}$. Combined with Lemma 1, we can derive the final expression of the CDF in the HDT protocol for the MRC and SC theories as follows:

$$F_{T_k^{(\mathrm{MRC})}}(t) = \frac{2}{\Gamma(M)}\left(\frac{\Psi(t)\mathscr{K}_{k1}}{\omega_k\Theta_k}\right)^{\frac{M}{2}} K_M\left(2\sqrt{\frac{\Psi(t)\mathscr{K}_{k1}}{\omega_k\Theta_k}}\right), \tag{19}$$

$$\begin{aligned} F_{T_k^{(SC)}(t)} &= 2M\sum_{m=0}^{M-1}\binom{M-1}{m}(-1)^{m)} \\ &\times\sqrt{\frac{\Psi(t)\mathscr{K}_{k1}}{(m+1)\omega_k\Theta_k}}K_1\left(2\sqrt{\frac{(m+1)\Psi(t)\mathscr{K}_k}{\omega_k\Theta_k}}\right), \end{aligned} \tag{20}$$

where $\Psi(t) = \exp(\frac{\mathscr{B}_k}{t}) - 1$, and the packet outage probability of a single sensor node for the HDT protocol can be derived combining (19) and (20) as follows:

$$\mathscr{O}_k^{(MRC)} = 1 - F_{T_k^{(MRC)}}(t_{out}), \tag{21}$$

$$\mathscr{O}_k^{(SC)} = 1 - F_{T_k^{(SC)}}(t_{out}). \tag{22}$$

4.1.2. System Performance Analysis of the HDT Protocol Scheme

Because the transmission time of each sensor node in the HDT protocol is independent of one another, the CDF of $T_{max}^{(v)}$ and $T_{min}^{(v)}$ can be expressed as follows:

$$\begin{aligned} F_{T_{\max}^{(v)}}(t) &= \Pr\left\{\max_{k\in\{1,2,\ldots,K\}}\left\{T_k^{(v)}\right\} < t\right\} \\ &= \prod_{k=1}^{K} F_{T_k^{(v)}}(t), \end{aligned} \tag{23}$$

$$\begin{aligned} F_{T_{\min}^{(v)}(t)} &= \Pr\left\{\min_{k\in\{1,2,\ldots,K\}}\left\{T_k^{(v)}\right\} < t\right\} \\ &= 1 - \prod_{k=1}^{K}\left(1 - F_{T_k^{(v)}}(t)\right). \end{aligned} \tag{24}$$

The system reliability has been defined in (14), and combining (23), we can re-deduce the definition of the system reliability of the HDT protocol as follows:

$$\mathscr{R}^{(v)} = F_{T_{\max}^{(v)}}(t_{out}) = \prod_{k=1}^{K} F_{T_k^{(v)}}(t_{out}). \tag{25}$$

Through formula (15), we can easily derive the expression of the outage probability of the HDT protocol as follows:

$$\begin{aligned} \mathscr{O}_{sys}^{(v)} &= 1 - F_{T_{\min}^{(v)}}(t_{out}) \\ &= \prod_{k=1}^{K}\left(1 - F_{T_k^{(v)}}(t_{\mathrm{out}})\right), \quad v \in \{MRC, SC\}. \end{aligned} \tag{26}$$

4.2. The Analysis of HHT Protocol

4.2.1. Packet Timeout Probability Analysis of Single Node

Analogously, we need to derive the CDF of the packet transmission time for the HHT protocol. Combining (6) with (11) and (12), the CDF of time $T_k^{(v)}$ in the HHT protocol can be rewritten as follows:

$$F_{T_k^{(v)}}(t) = \Pr\left\{G_{k1}^{(v)}G_{k3} \le \Psi(t)\mathscr{K}_{k2}\right\}, \tag{27}$$

where $\mathscr{H}_{k2} = \frac{d_k^{-2\lambda}(1-\alpha)_k}{\alpha_{0k}\gamma_0\eta_k\mu_k}$. Similarly, using (27), in combination with Lemma 1, we can easily deduce the expression of the CDF in the HHT protocol for the MRC and SC theories as follows:

$$F_{T_k^{(\mathrm{MRC})}}(t) = \frac{2}{\Gamma(M)}\left(\frac{\Psi(t)\mathscr{H}_{k2}}{\omega_k\Phi_k}\right)^{\frac{M}{2}} K_M\left(2\sqrt{\frac{\Psi(t)\mathscr{H}_{k2}}{\omega_k\Phi_k}}\right), \tag{28}$$

$$\begin{aligned} F_{T_k^{(SC)}}(t) &= 2M\sum_{m=0}^{M-1}\binom{M-1}{m}(-1)^m \\ &\times\sqrt{\frac{\Psi(t)\mathscr{H}_{k2}}{(m+1)\omega_k\Phi_k}}K_1\left(2\sqrt{\frac{(m+1)\Psi(t)\mathscr{H}_k}{\omega_k\Phi_k}}\right). \end{aligned} \tag{29}$$

The packet outage probability of single sensor node for the HHT protocol can be derived by combining (28) with (29) and using (15) as

$$\mathscr{O}_k^{(MRC)} = 1 - F_{T_k^{(MRC)}}(t_{out}), \tag{30}$$

$$\mathscr{O}_k^{(SC)} = 1 - F_{T_k^{(SC)}}(t_{out}). \tag{31}$$

4.2.2. System Performance Analysis of the HHT Protocol Scheme

The system reliability has been defined in (14). We can re-deduce the definition of the system reliability for HHT as follows:

$$\mathscr{R}^{(v)} = F_{T_{\max}^{(v)}}(t_{out}) = \prod_{k=1}^{K} F_{T_k^{(v)}}(t_{\mathrm{out}}). \tag{32}$$

Similarly, using the definition of outage probability in (14), we can rewrite the outage probability of HHT protocol as

$$\begin{aligned} \mathscr{O}_{\mathrm{sys}}^{(v)} &= 1 - F_{T_{\min}^{(v)}(t_{\mathrm{out}})} \\ &= \prod_{k=1}^{K}\left(1 - F_{T_k^{(v)}}(t_{\mathrm{out}})\right), \quad v \in \{MRC, SC\}. \end{aligned} \tag{33}$$

5. Numerical Results

This section presents the analysis and simulation results for our system. We focus on evaluating our proposed performance metrics, which include the system reliability, packet timeout probability, and outage probability for both the HHT and HDT protocols. Due to the randomness of the channel state, we use Monte Carlo simulation technology for our analysis. To ensure accuracy, we sample a total of 10^5 loops, and the system parameters are set according to Table 1.

Table 1. The default parameters employed in this paper to simulate the system we consider.

The packet size of HDT protocol	$L_1 = K * 512$ bits
The packet size of HHT protocol	$L_2 = 512$ bits
The time of timeout threshold	$t_{out} = 0.864$ ms [22]
Bit error rate	$BER = 10^{-2}$ [22]
Channel mean gains	$\omega_k = \Theta_k = \Phi_k = 1$ [22]
The locates of BS	$(x_0, y_0) = (0, 0)$
The pathloss exponent of channel	$\lambda = 4$ [22]

In Figure 4, we analyze the impact of different distances between the BS and the sensor nodes on the packet timeout probability. We set the coordinates of the four nodes as $(x_1, y_1) = (0.6, 0.6)$, $(x_2, y_2) = (0.55, 0.55)$, $(x_3, y_3) = (0.5, 0.5)$, and $(x_4, y_4) = (0.45, 0.45)$. The energy-harvesting time of the HHT protocol is $\alpha_{0k} = 0.05$, while that of the HDT protocol is $\alpha_0 = 0.2$. The packet transmission time for both protocols is $(1 - \alpha)_k = 0.2$. According to our observation, node 4 performs the best out of all nodes, due to its lowest packet timeout probability. This is the case since node 4 can harvest the most energy and has more energy available for packet transmission because of the fact that the distance between it and the BS is the shortest. Furthermore, we note that the packet timeout probability under the HHT protocol is consistently lower than that under the HDT protocol for all nodes. At the same time, under the same conditions, the packet timeout probability using MRC technology is lower than that using SC technology. This is because MRC selected the maximum value of channel gain, which has a higher channel gain than the average value of channel gain selected by SC. Additionally, the packet timeout probability of the MRC technology in the HHT protocol is lower than that of the SC technology in the HHT protocol, and the system performance of the HHT protocol using MRC technology is the best under the same distances.

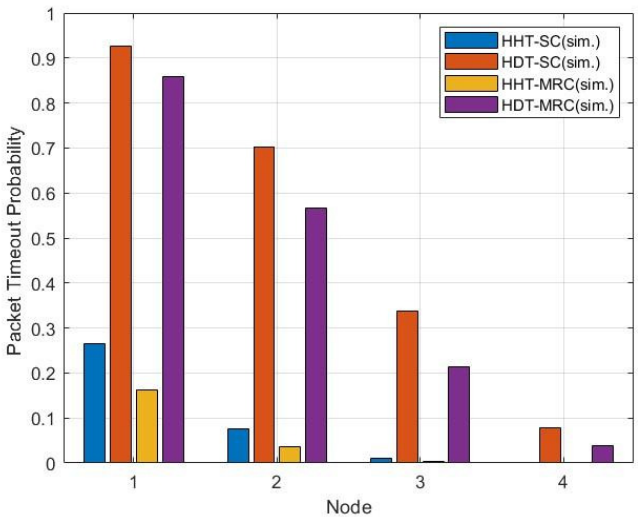

Figure 4. The impact of different distances between the BS and the sensor nodes on the packet timeout probability.

In Figure 5, we examine the impact of energy harvesting effectiveness between single sensors on the packet outages probability for the system. According to [22], we set the coordinates of the sensor nodes to a fixed point $(x_k, y_k) = (0.6, 0.6)$. We adopt the univariate research concept and set the number of antennas and nodes as $M = 2$ and $K = 4$, respectively. We assign four different energy harvesting efficiencies to four sensor nodes, namely $\eta_1 = 0.2$, $\eta_2 = 0.3$, $\eta_3 = 0.4$, and $\eta_4 = 0.5$. Additionally, the energy-harvesting times for the HDT protocol and the HHT protocol are denoted as $\alpha_{0k} = 0.05$ and $\alpha_0 = 0.2$, respectively. Our observations indicate that increasing the energy harvesting efficiency leads to a decrease in the packet timeout probability for both the HHT and HDT protocols. This is because higher energy-harvesting efficiency allows sensor nodes to harvest more energy, which in turn enables them to use more energy for information transmission. This reduces the packet loss rate and leads to improved system performance. Moreover, we have observed that the packet timeout probability of the HHT protocol is consistently lower than that of the HDT protocol under the same energy harvesting efficiency conditions. This can be attributed to the fact that the HHT protocol uses a more refined time slot division and is therefore more sensitive to channel variations. Thus, the performance of the HHT protocol is generally better than that of the HDT protocol under similar conditions.

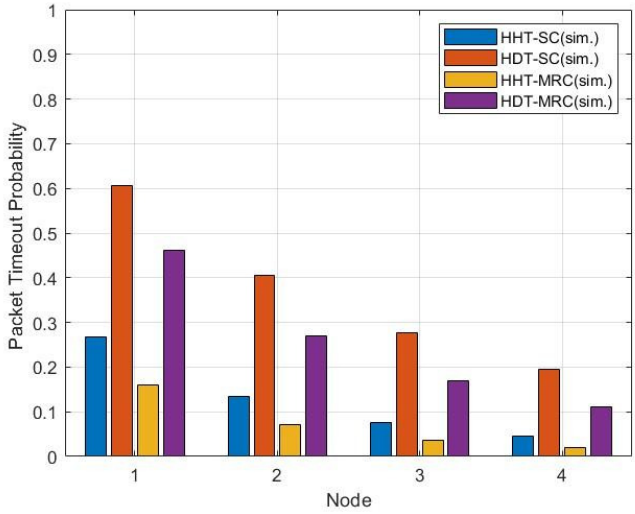

Figure 5. The impact of harvesting efficiency coefficients on the packet timeout probability.

In Figure 6, we investigate the system reliability of the HHT and HDT protocols. where the information transmission time is $(1-\alpha)_k = 0.19$, the coordinates of the sensor nodes are set to $(x_k, y_k) = (0.3, 0.3)$ [22], and the energy-harvesting time for the HHT protocol and the HDT protocol is $\alpha_{0k} = 0.01$ and $\alpha_0 = 0.05$, respectively, and the energy-harvesting efficiency is $\eta_k = 0.5$. The figure clearly indicates that as SNR γ_0 increases, so does the system reliability. This is because an increase in SNR results in more energy being harvested by sensor nodes, which is then used for uplink information transmission, resulting in improved system performance. Furthermore, we observe that the system reliability of the HHT protocol is higher than that of the HDT protocol at the same SNR. This is due to the fact that the HHT protocol harvests energy at the head of each segment, which is less affected by channel status than the HDT protocol, which harvests energy at the head of the total period. Similarly, we also found that under the condition of HHT protocol, the system reliability using MRC technology is better than that of using SC technology. This is because the MRC selects the maximum value of the channel gain, which has a higher channel gain than the average value of the channel gain selected by the SC, which results in the system being able to harvest more energy for information transmission. We can also observe that increasing the number of antennas from $M = 2$ to $M = 3$ increases system reliability by utilizing the HDT protocol with MRC technology.

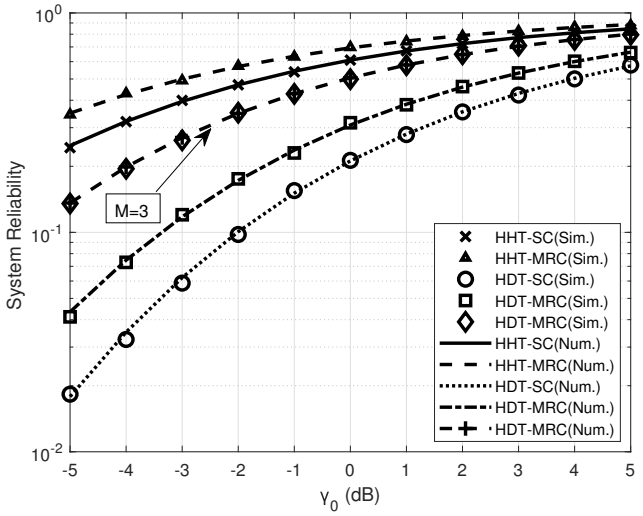

Figure 6. The simulation results of the impact of the SNR on system reliability.

Figure 7 depicts the impact of energy-harvesting time length on the system reliability of the HHT and HDT protocols in the complete system. We fix energy-harvesting efficiency as $\eta_k = 0.5$, and the coordinates of the sensor nodes are set to $(x_k, y_k) = (0.3, 0.3)$. The figure shows that extending the energy-harvesting time increases the system reliability. This is because the sensor nodes can obtain more energy from the BS, reducing the data packet loss rate during data transmission and improving system performance. Furthermore, we have consistently observed that the HHT protocol outperforms the HDT protocol in terms of system reliability regardless of the energy-harvesting time length. This is because the HHT protocol uses a more reasonable time allocation method, allocating energy-harvesting time at the head of each time slot, and is less affected by complex channel environments. Additionally, the HHT protocol utilizes MRC technology, which results in the highest system reliability and best system performance.

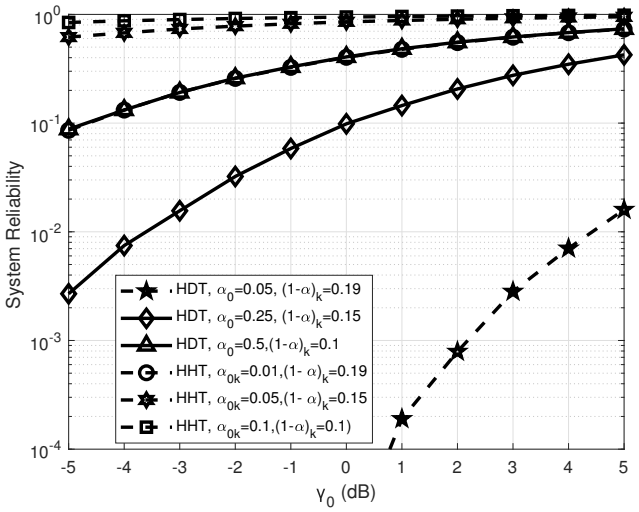

Figure 7. The simulation results of the impact of energy harvesting time on system reliability.

Figure 8 shows how the energy-harvesting efficiency coefficient affects the probability of a system outage in our wireless communication system. Specifically, we fix the energy-harvesting time for the HHT and HDT protocols at $\alpha_{0k} = 0.01$ and $\alpha_0 = 0.05$, respectively, and set the information transmission time as $(1 - \alpha)_k = 0.19$. The energy-harvesting efficiency is held constant at $\eta_k = 0.5$. Our simulation results demonstrate that increasing the energy-harvesting efficiency leads to a continuous decrease in the outage probability in our wireless communication system, as shown in Figure 8. Furthermore, the HHT protocol consistently outperforms the HDT protocol in terms of lower outage probability. This superiority can be attributed to the fact that the HHT protocol harvests energy at the beginning of each time slot, which is less susceptible to channel fading. Consequently, more energy is available for information transmission, resulting in a reduced outage probability. Additionally, we discovered that when the number of antennas is increased from $M = 2$ to $M = 3$, the probability of a packet outage is greatly reduced because doing so enables the system to obtain greater diversity gain. Therefore, based on our simulation results, we can conclude that the HHT protocol is a preferable option for energy harvesting in wireless communication systems, as it achieves better system performance compared to the HDT protocol.

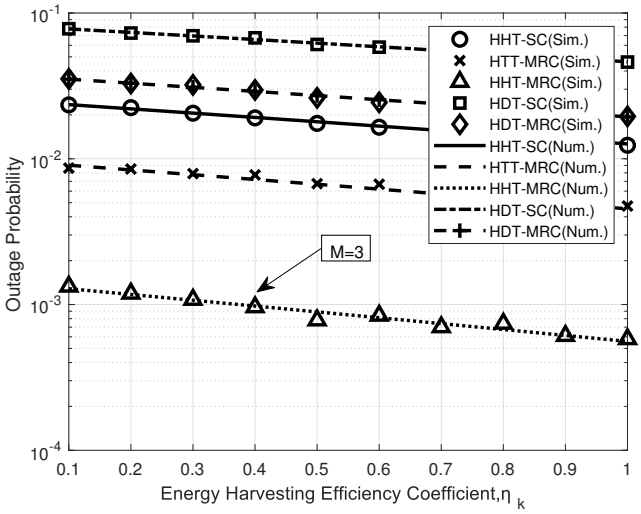

Figure 8. The simulation results of the impact of the energy-harvesting efficiency coefficient on the packet outage probability.

6. Conclusions

In this paper, we present a system model for energy harvesting and information transmission in wireless communication, which utilizes two protocols in the energy-harvesting part of the downlink, namely the HHT and HDT protocols. Our main objective is to compare and analyze the system reliability, packet timeout probability, and outage probability of these two protocols to evaluate their performance. Moreover, we simulate the proposed system using the Monte Carlo simulation method based on the channel state. Our simulation results indicate that the HHT protocol outperforms the HDT protocol in terms of system reliability, packet timeout probability, and outage probability. Specifically, the HHT protocol demonstrates higher system reliability and lower packet timeout and outage probabilities compared to the HDT protocol under similar conditions. Therefore, the HHT protocol with MRC technology is considered optimal for our proposed system.

In our future work, we plan to apply our research results to artificial hearts and other medical fields, which may lead to unexpected benefits. This could potentially alleviate the current limitations for artificial heart recipients who are hesitant to venture far from urban areas due to concerns about timely energy replenishment as well as improve their quality of life. Additionally, the effective utilization of RF energy harvesting could bring new changes to our 6G smart era and provide a new way for people to experience the relative abundance of energy in their daily lives.

Author Contributions: Conceptualization, K.L. and Z.Z.; methodology, K.L.; software, K.L.; validation, K.L. and Z.Z.; formal analysis, K.L.; investigation, K.L.; resources, Z.Z.; data curation, K.L.; writing—original draft preparation, K.L.; writing—review and editing, Z.Z.; visualization, K.L.; supervision, Z.Z.; project administration, Z.Z. All authors have read and agreed to the published version of the manuscript.

Funding: This research received no external funding.

Data Availability Statement: Not applicable, the study does not report any data.

Conflicts of Interest: The authors declare no conflict of interest.

References

1. Dang, S.; Alouini, M.S.; Shihada, B. Pre-6G Graduate Education of Communications Engineering. *Front. Commun. Netw.* **2022**, *2*, 798–880. [CrossRef]
2. Alcalá-Garrido, H.A.; Barrera-Figueroa, V.; Rivero-Ángeles, M.E.; García-Tejeda, Y.V.; Pérez, H.R. Analysis and Design of a Wireless Sensor Network Based on the Residual Energy of the Nodes and the Harvested Energy from Mint Plants. *J. Sens.* **2021**, *2021*, 6655967. [CrossRef]

3. Olatinwo, S.O.; Joubert, T.H. Efficient energy resource utilization in a wireless sensor system for monitoring water quality. *EURASIP J. Wirel. Commun. Netw.* **2019**, *2019*, 6. [CrossRef]
4. Prakasam, P.; Kumar, T.R.S.; Velmurugan, T.; Nandakumar, S. Efficient power distribution model for IoT nodes driven by energy harvested from low power ambient RF signal. *Microelectron. J.* **2020**, *95*, 46–65. [CrossRef]
5. Chincoli, M.; Liotta, A. Self-learning power control in wireless sensor networks. *Sensors* **2018**, *18*, 375. [CrossRef] [PubMed]
6. Marriwala, N. Energy harvesting system design and optimization using high bandwidth rectenna for wireless sensor networks. *Wirel. Pers. Commun.* **2022**, *122*, 669–684. [CrossRef]
7. Tran, H.; Uhlemann, E.; Truong, Q. X.; So-In, C.; Balador, A. Reliable communication performance for energy harvesting wireless sensor networks. In Proceedings of the 2019 IEEE 89th Vehicular Technology Conference (VTC2019-Spring), Kuala Lumpur, Malaysia, 28 April–1 May 2019.
8. Kulshrestha, J.; Mishra, M.K. Energy balanced data gathering approaches, issues and research directions. *Telecommun. Syst.* **2021**, *76*, 299–327. [CrossRef]
9. Amer, A.A.G.; Sapuan, S.Z.; Nasimuddin, N.; Alphones, A.; Zinal, N.B. A comprehensive review of metasurface structures suitable for RF energy harvesting. *IEEE Access* **2020**, *8*, 76433–76452. [CrossRef]
10. Vu, H.S.; Nguyen, N.; Ha-Van, N.; Seo, C.; Le, M.T. Multiband ambient RF energy harvesting for autonomous IoT devices. *IEEE Microw. Wirel. Components Lett.* **2020**, *30*, 1189–1192. [CrossRef]
11. Wagih, M.; Weddell, A.S.; Beeby, S. Rectennas for radio-frequency energy harvesting and wireless power transfer: A review of antenna design [antenna applications corner]. *IEEE Antennas Propag. Mag.* **2020**, *62*, 95–107. [CrossRef]
12. Mukhopadhyay, S.C.; Tyagi, S.K.S.; Suryadevara, N.K.; Piuri, V.; Scotti, F.; Zeadally, S. Artificial intelligence-based sensors for next generation IoT applications: A review. *IEEE Sens. J.* **2021**, *21*, 9215–9226. [CrossRef]
13. Shen, S.; Zhang, Y.; Chiu, C.-Y.; Murch, R. A triple-band high-gain multibeam ambient RF energy harvesting system utilizing hybrid combining.*IEEE Trans. Ind. Electron.* **2021**, *67*, 24920–24932. [CrossRef]
14. Alevizos, P.N.; Bletsas, A. Sensitive and nonlinear far-field RF energy harvesting in wireless communications. *IEEE Trans. Wirel. Commun.* **2018**, *17*, 3670–3685. [CrossRef]
15. Clerckx, B.; Zhang, R.; Schober, R.; Ng, D.W.K.; Kim, D.I.; Poor, H.V. Fundamentals of wireless information and power transfer: From RF energy harvester models to signal and system designs. *IEEE J. Sel. Areas Commun.* **2015**, *37*, 4–33. [CrossRef]
16. Alzahrani, B.; Ejaz, W. Resource management for cognitive IoT systems with RF energy harvesting in smart cities.*IEEE Access* **2018**, *6*, 62717–62727. [CrossRef]
17. Li, H.; Ota, K.; Dong, M. Energy cooperation in battery-free wireless communications with radio frequency energy harvesting. *ACM Trans. Embed. Comput. Syst. (TECS)* **2018**, *17*, 1–17. [CrossRef]
18. Luo, Y.; Pu, L.; Wang, G.; Zhao, Y. RF energy harvesting wireless communications: RF environment, device hardware and practical issues. *Sensors* **2019**, *19*, 3010. [CrossRef]
19. Khairy, S.; Han, M.; Cai, L.X.; Cheng, Y. Sustainable wireless IoT networks with RF energy charging over Wi-Fi (CoWiFi). *IEEE Internet Things J.* **2019**, *6*, 10205–10218. [CrossRef]
20. Singh, A.; Singh, D.P. Enhancing the Performance of Leach Protocol in Wireless Sensor Network. *Int. J. Comput. Appl.* **2015**, *122*, 11. [CrossRef]
21. Vo, V.N.; Nguyen, T.G.; So-In, C.; Tran, H. Outage performance analysis of energy harvesting wireless sensor networks for NOMA transmissions. *Mob. Netw. Appl.* **2020**, *25*, 23–41. [CrossRef]
22. Tran, H.; Åkerberg, J.; Björkman, M.; Tran, H.-V. RF energy harvesting: An analysis of wireless sensor networks for reliable communication. *Wirel. Netw.* **2017**, *25*, 185–199. [CrossRef]